Supporting Information

An electron-accepting half-sandwich iridium(III) complex for the treatment of hypoxic tumors via synergetic chemo- and phototherapy

Yuliang Yang[a], Ya Gao[a], Jian Zhao[a,b]*, Shaohua Gou[a,b]*

[a]Pharmaceutical Research Center and School of Chemistry and Chemical Engineering, Southeast University, Nanjing 211189, China

[b]Jiangsu Province Hi-Tech Key Laboratory for Biomedical Research, Southeast University, Nanjing 211189, China

*Corresponding author. E-mail addresses: zhaojianzhaokuan@163.com (J. Zhao), 2219265800@qq.com (S. Gou)

Contents

Experimental section……. S2-S8.

Figure S1-S16……S9-S16.

Table S1……S16.

References……S16.

EXPERIMENTAL SECTION

Materials

All common chemicals and solvents were of analytical reagent grade purity and obtained from a local chemical company (Nanjing Wan Qing Co., Ltd. China) and used without further purification. 9,10-Anthracenediyl-bis-(methylene) dimalonic acid (ABDA), methylene blue (MB) and nicotinamide adenine dinucleotide (NADH) were obtained from Sigma-Aldrich. Apoptosis inhibitor (z-VAD-FMK), necrostatin-1 (Nec-1), ferrostatin-1 (Fer-1), deferoxamine (DFO) and 3-methyladenine (3-MA) were purchased from Bide Pharmatech Ltd. C11-BODIPY was provided from Cayman Chemical. Detailed information of detection kits used in this study are listed as follows: Calcein-AM/PI Double Stain Kit was obtained from KeyGEN BioTECH Corp., Ltd. Intracellular $O_2^{-\bullet}$ assay kit dihydroethidium (DHE) was purchased from Shanghai Macklin Biochemical Co., Ltd. Hypoxia/Oxidative Stress Detection Kit, ROS-ID™, was provided from Enzo Life Sciences Inc. NAD/NADH Assay Kit (Colorimetric) was obtained from Abcam (ab65348). Methylthiazolyldiphenyl-tetrazolium bromide (MTT), Reactive Oxygen Species Assay Kit (DCFH-DA), GSH and GSSG Assay Kit, Annexin V-FITC Apoptosis Detection Kit, Mitochondrial Membrane Potential Assay Kit (JC-1) and ATP Assay Kit were purchased from Beyotime Biotechnology. Singlet Oxygen Fluorescence Probe (SOSG) and Hydroxyphenyl Fluorescein (HPF) were got from Nantong Feiyu Biotechnology Co., LTD. Mouse breast cancer cell line (4T1) and normal hepatic cell line (L02) were offered from Jiangsu Keygen Biotech Corp., Ltd. RPMI-1640 medium, fetal bovine

serum (FBS), glutamine and penicillin/streptomycin were commercially available from Sigma Aldrich.

Instruments

All NMR spectra were measured on a Bruker Avance III-HD 600 MHz spectrometer. UV-vis spectra were recorded on a Shimadzu UV2600 instrument and Fluorescence spectra were measured on a SHIMADZU RF-6000 fluorometer. Mass spectrometry was performed on an Agilent 6224 ESI/TOF MS instrument. Microanalysis (C, H, and N%) was carried out using a Carlo Erba model EA 1108 microanalyzer. Cyclic voltammetry (CV) was performed with a CorrTest CS350 electrochemical workstation (Corrtest Instruments Co., Ltd., China). Confocal imaging was performed on an Olympus FV1000 confocal microscope (Olympus, Japan). The apoptosis was detected by flow cytometry (BD Bioscience FACS Calibur) and the results were analyzed by ModFit Software. 635 nm laser source was used for light irradiation.

Photocatalytic reactions of Ir-NDI with NADH by UV-visible spectroscopy. Reactions between the **Ir-NDI** and NADH at different ratios were monitored by UV-vis at 310 K in the dark or upon photo-irradiation with 635 nm light (145 mW cm^{-2}). The concentration of NADH was obtained using the extinction coefficient ε_{339} = 6220 $M^{-1}\cdot cm^{-1}$. The catalytic turnover of NAD^+ was calculated using the following equations:

$[NAD^+] = [Abs(339\ nm)_{initial} - Abs(339\ nm)_{final}]/Abs(339\ nm)_{initial} \times [NADH]$

Turnover number (TON) = $[NAD^+]/[Catalyst]$

Turnover frequency (TOF) = Turnover number/time (h)

Photocatalytic oxidation of NADH by ^{1}H NMR spectra. NADH (3.5 mM) was added to an NMR tube containing 5 μM of **Ir-NDI** in 80% CD_3OD/20% D_2O. ^{1}H NMR spectra of the resulting solutions were recorded at 298 K after 10 min light irradiation (635 nm, 145 mW cm^{-2}) or leave it in the dark for 1 h.

Cyclic Voltammetry. Cyclic voltammograms of **Ir-NDI** was conducted by using three-electrode system. A platinum-carbon compound electrode was used as working electrode, the Pt wire electrode and the Ag/Ag^+ electrode were used as the auxiliary electrode and reference electrode, respectively. The measurement was conducted according to previously reported literature.[1] The ferrocene/ferrocenium redox couple (F_C^+/F_C) was used as an external standard. $E_{1/2}(F_C^+/F_C)$ is the half-wave potential of the F_C^+/F_C. The scan range was determined from -1.5 V to 1.5 V and the scan rate was optimized as 50 mV/s.

Cell Lines and Culture Media. 4T1 cells and L02 cells were cultured with RPMI-1640 medium, which were supplemented with 10% fetal bovine serum (FBS), and 100 U/mL penicillin−streptomycin. The cells were grown in a humidified atmosphere of 5% CO_2 at 37 °C. Mitsubishi™ AnaeroPack-Anaero (Japan) gas generator was used for cultivation of cells under hypoxic environment. Oxygen indicator was used to detect the oxygen levels in the chamber (1 % O_2).

Cellular NADH determination experiments. NADH changes in 4T1 cells exposed to different concentrations of **Ir-NDI** were performed using the NAD^+/NADH assay kit provided by Abcam (ab65348). In brief, 5×10^4 4T1 cells per well were cultured

in six-well plates at 37 ℃ in a humidified, 5% CO_2 atmosphere for 24 h. After that, the cells were exposed to different concentrations of **Ir-NDI**, i.e., 0, 5, 10, 15, and 20 μM. 8 h later, light irradiation with 635 nm light source was performed (145 mW cm^{-2}, 10 min) and cells were allowed to recover for 4 h at 37 ℃. For NAD^+/NADH extraction, the medium was removed by suction and cells were harvested by scraping, followed by washing with cold PBS buffer and spinning at 2,000 rpm (5 min) to get the cell pellets. Cell pellets were then extracted using NAD^+/NADH extraction buffer, and the samples were filtered by a 10 KD Spin Column so as to remove the intracellular enzymes which could consume NADH rapidly. After heating the collected filtrate at 60 ℃ for 0.5 h in a water bath, cellular NADH content was finally quantified according to the manufacturer's instructions.

Depletion of GSH in solution. The consumption of GSH was monitored by UV-vis spectroscopy. **Ir-NDI** (10 μM) was mixed with GSH (200 μM) at room temperature. At different irradiation time points, 250 μL of this solution was added into 2250 μL PBS, and then 10 μL 5,5'-dithiobis-(2-nitrobenzoic acid) (DTNB) (10 mg/mL) was added. The absorbance spectrum of the supernatant was measured by UV-vis spectroscopy.

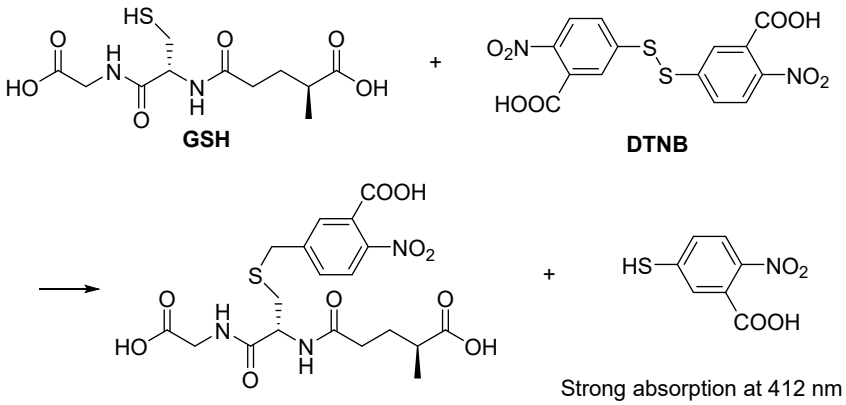

Cellular GSH detection. **Ir-NDI**-induced GSH concentration variation was determined by using a GSH and GSSG Assay Kit (Beyotime). The 4T1 cells (1×10^7) in a 13 cm culture dish were treated by **Ir-NDI** at a dose of 10 μM in the dark or under light irradiation (635 nm, 145 W cm^{-2}, 10 min). The incubation time was set at 8 h and drugs-free cells were used as the control. Then the cellular GSH concentrations of three groups 10 μM (**Ir-NDI**-Dark and **Ir-NDI**-Light) and Control were measured according to the manufacturer's suggested protocol.

Intracellular lipid peroxides measurement. 4T1 cells were incubated with **Ir-NDI** **(**10 μM) or **Ir-NDI +** Fer-1 (10 μM + 10 μM) for 8 h followed by incubation with 30 μM C11-BODIPY for 30 min. After that, cells were washed with PBS and then irradiated with 635 nm red light for 10 min at a power density of 145 mW cm^{-2}. The green fluorescence was immediately observed using CLSM with the excitation wavelength of 488 nm, and emission collection wavelength from 520 nm to 620 nm.

GPX4 analysis. 4T1 cells were seeded in 6-well plates at a density of 4×10^5 per well. After 24 h, **Ir-NDI** was added at a dose of 10 μM for 8 h incubation, the cells were irradiated (635 nm, 145 mW cm^{-2}) for 10 min. The cells without light irradiation were used as control. All cells were collected. The expression of GPX4 in 4T1 cells upon formulation treatment was analyzed by western blotting according to the protocol method. The cell lysates containing identical protein (40 μg) were subjected to standard electrophoresis, followed by antibody incubation at 4 °C. The dilution ratio for the first antibody was 1:2000 (β-actin-specific antibody) and 1:2500 (GPX4-specific antibody). Regarding the secondary antibody, the dilution ratio was 1: 5000

for both GPX4 and β-actin. The protein bands were developed via the ECLTM western blotting detection reagents.

Mitochondrial membrane potential. 4T1 cells were seeded in glass-bottomed cell culture dishes and incubated with **Ir-NDI** (10 μM) for 8 h at 37 °C with 5% CO_2. The cells were irradiated by 635 nm light (145 mW cm^{-2}) for 10 min and then treated with 1 μL JC-1 (5 μg/mL) at 37 °C for 20 min. The fluorescence intensity was measured by confocal microscopy in a red channel for J-aggregates (λ_{ex} = 488 nm, λ_{em} = 591−757 nm) and a green channel for JC-1 monomer (λ_{ex} = 488 nm, λ_{em} = 514−580 nm).

Annexin V-FITC/propidium iodide assay. 4T1 cells were seeded in glass-bottomed cell culture dishes and incubated with **Ir-NDI** (10 μM) for 8 h at 37 °C in 5% CO_2. The cells were then irradiated by 635 nm light (145 mW cm^{-2}) for 10 min and stained with 5 μL of annexin V-FITC for 40 min and 5 μL of propidium iodide for 10 min at room temperature in the dark. The samples were detected using a flow cytometer.

Animals and tumor model. All animal experiments involved in this study were approved by the Animal Care & Welfare Committee of Southeast University (Nanjing, China, permit no. SYXK2021-0022) and KeyGEN BioTECH Co. Ltd. (Nanjing, China, permit no. SYXK-20170040). In order to establish xenografted tumor models, BALB/c mice (female, 4-6 weeks, 16-18 g) were subcutaneously injected with 4T1 cell suspension (1×10^6 cells).

Mechanism of killing effect of Ir-NDI to 4T1 cells. 4T1 cells were pretreated with the following cell death pathway inhibitors for 30 minutes: 60 μM necrostatin-1 (Nec-1, necroptosis inhibitor); 20 μM Z-VAD-FMK (apoptosis inhibitor); 50 nM

ferrostatin-1 (Fer-1, ferroptosis inhibitor); 100 μM deferoxamine (DFO, ferroptosis inhibitor) and 100 μM 3-methyladenine (3-MA, autophagy inhibitor). Next, the cells were incubated with **Ir-NDI** (2 μM) for 8 h. Following treatment, the original cell culture medium was changed with fresh cell culture liquid. The 96-well cell-culture plate of the light group was irradiated by 635 nm laser (145 mW cm^{-2}) for 10 min. After light irradiation, plates were allowed to continue incubating for 40 h and then MTT reagent (25 μL/well, 5 mg/mL) was added into the wells. Four hours later, the liquid was disposed and DMSO (100 μL) was added, and the absorbance at 570 nm was recorded employing a microplate reader. Finally, IC_{50} values were calculated by cell viabilities under varying incubation doses. IC_{50} values expressed as mean ± s.d. (n = 3). For dark toxicity measurement, no laser irradiation was used to this assay, and all other steps were the same.

Statistical Analysis. *p*-Values were calculated after a *t* test against the control data. Data are expressed as the mean ± s.d. (number of experiments) and considered to be statistically significant at p values ≤ 0.05.

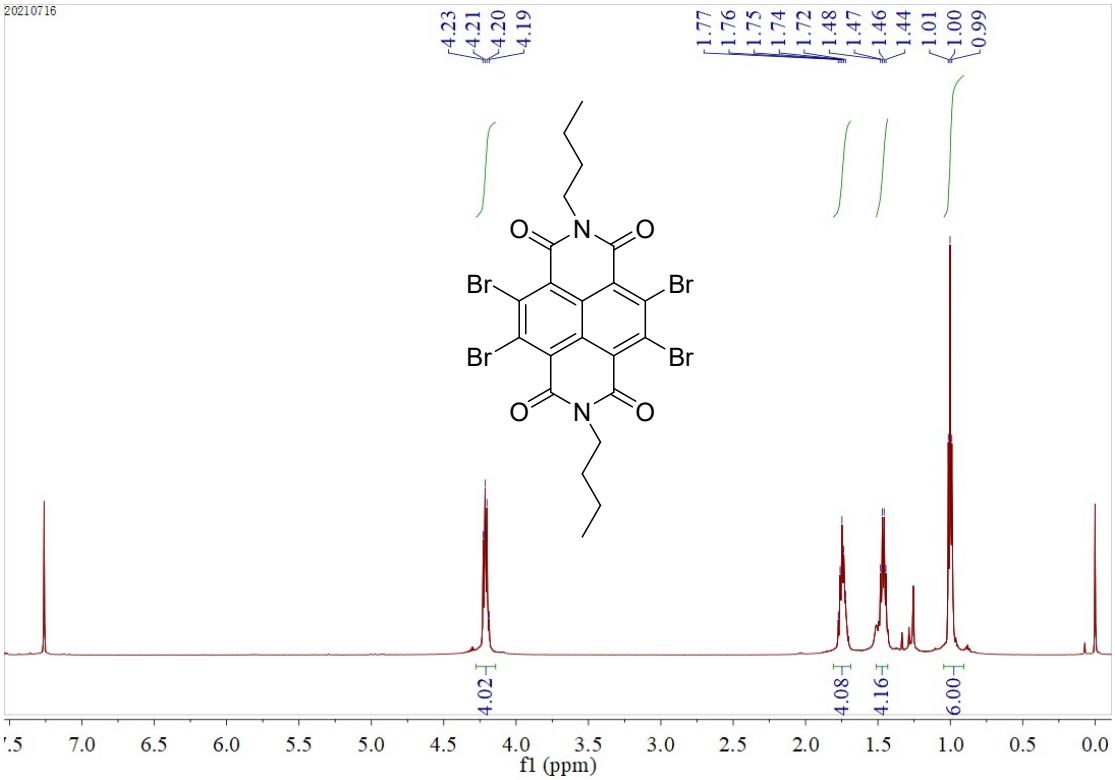

Fig. S1 ^{1}H NMR spectrum of **4BrNDA** in $CDCl_3$.

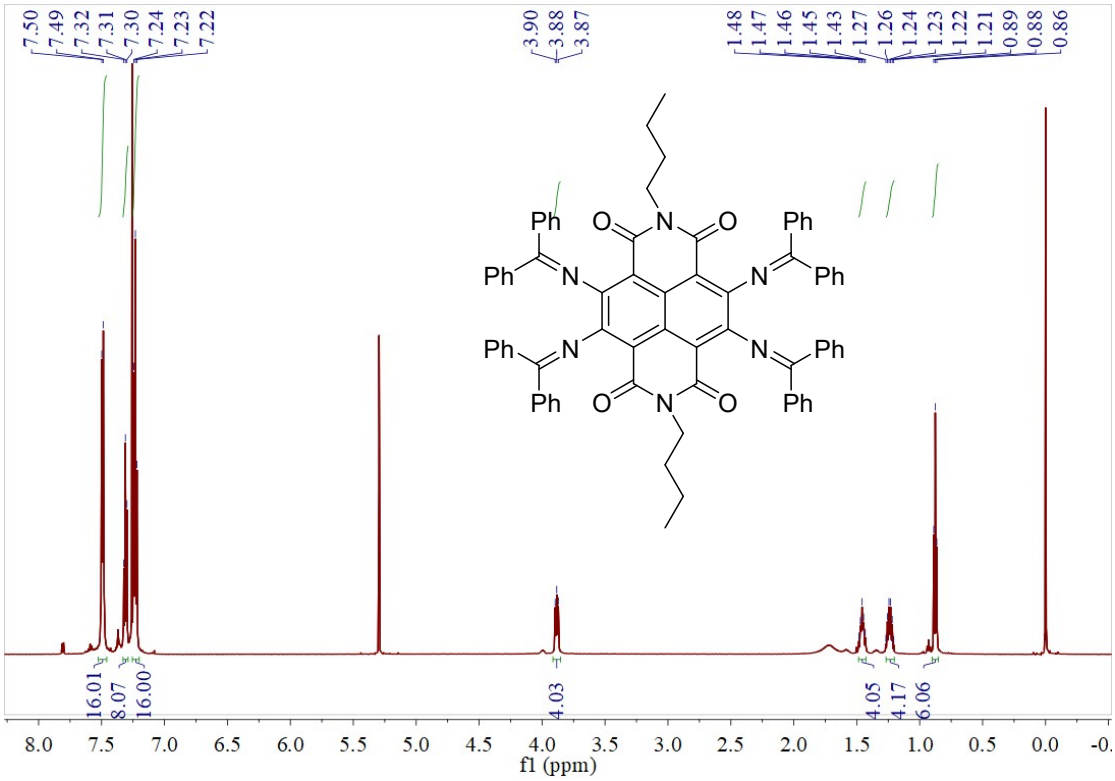

Fig. S2 ^{1}H NMR spectrum of **4NNDI** in $CDCl_3$.

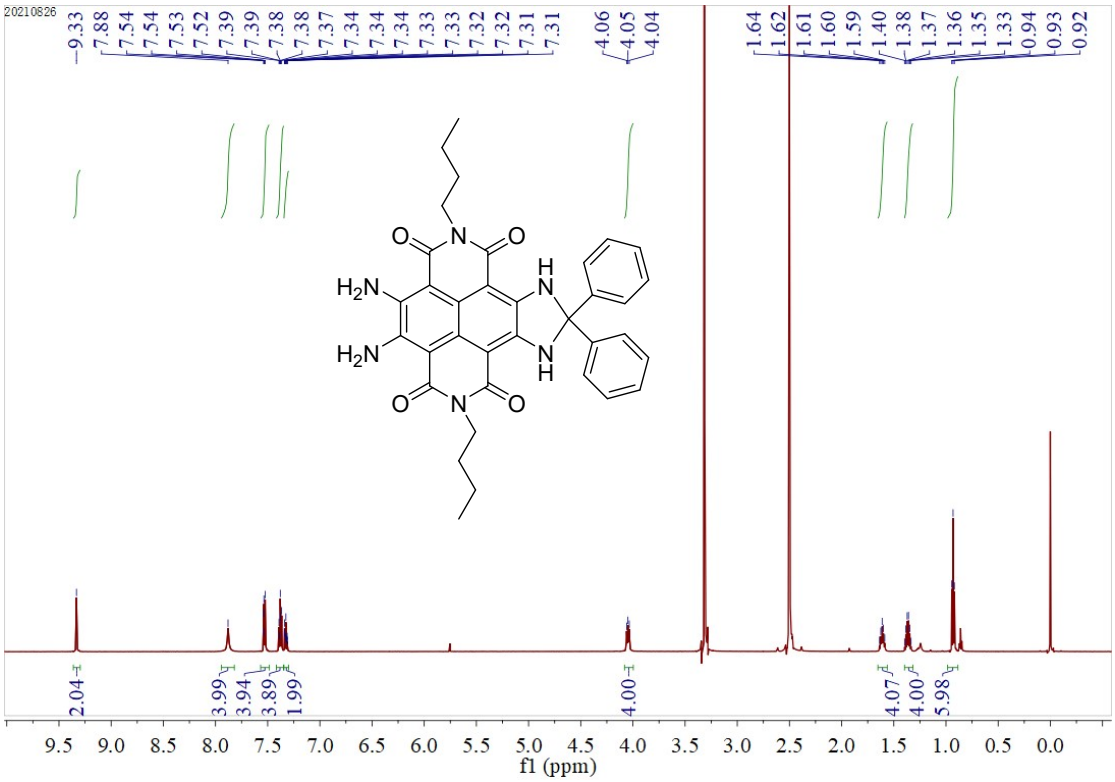

Fig. S3 ^{1}H NMR spectrum of **2NH$_2$-NDI** in DMSO-d_6.

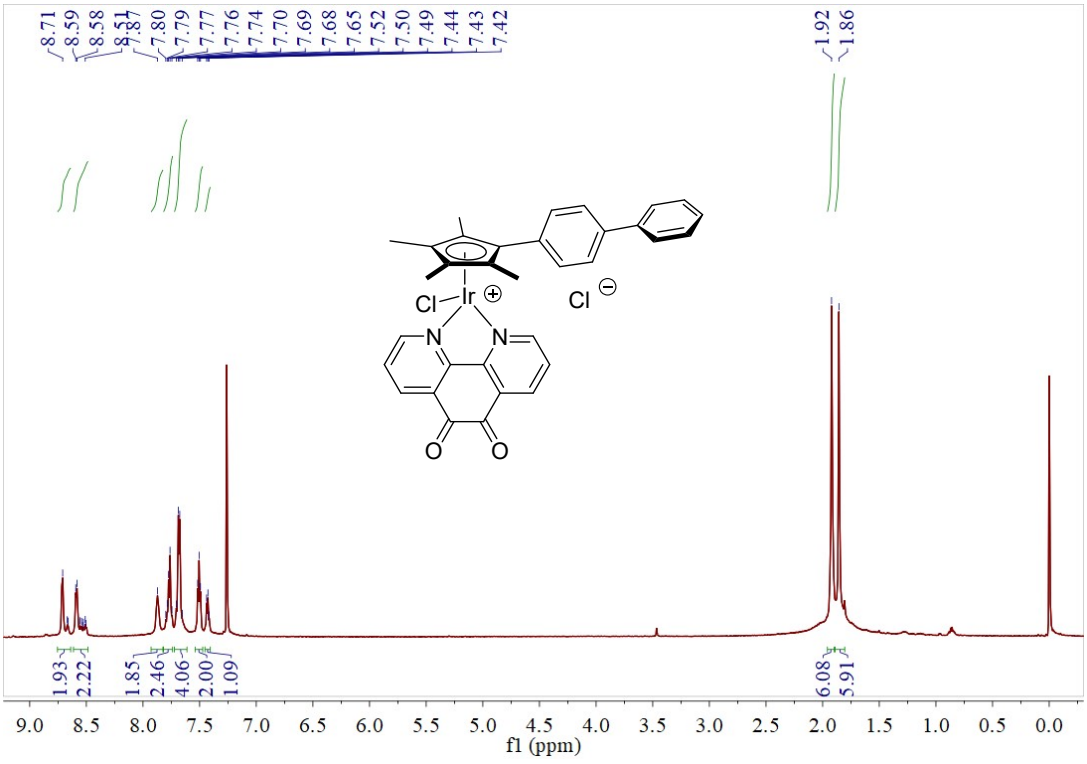

Fig. S4 ^{1}H NMR spectrum of [(η^5-Cp^{xbiph})Ir(phen-dione)Cl]Cl in $CDCl_3$.

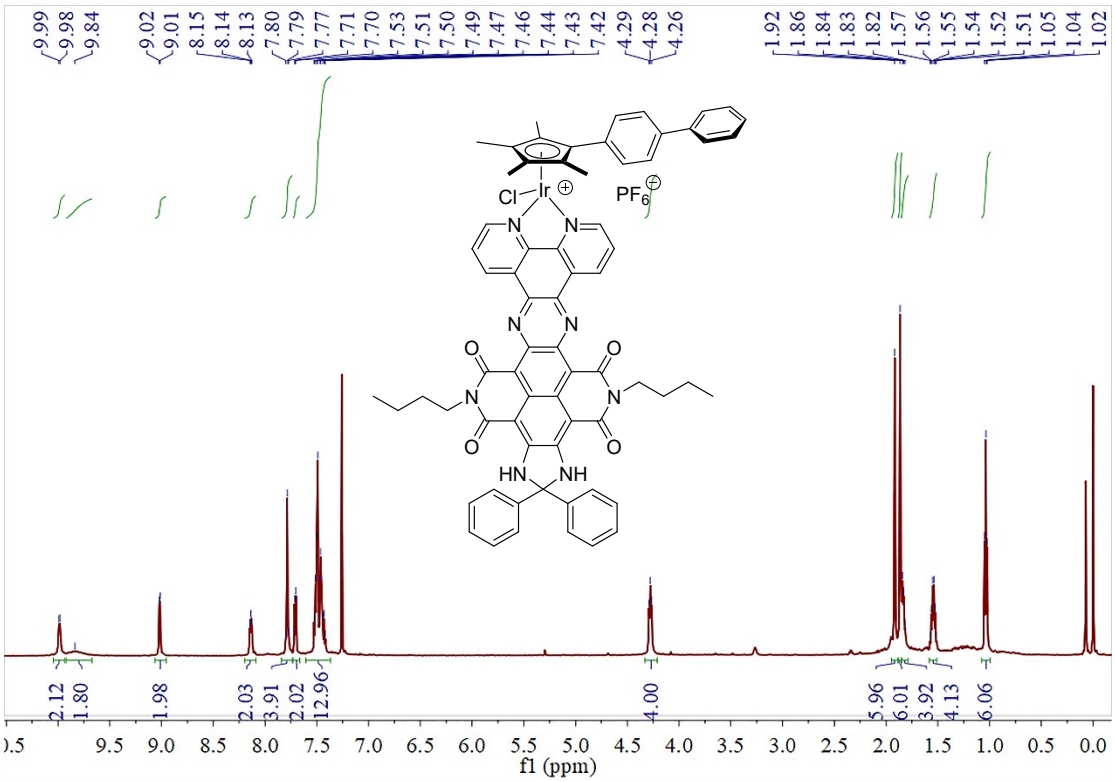

Fig. S5 ^{1}H NMR spectrum of **Ir-NDI** in $CDCl_3$.

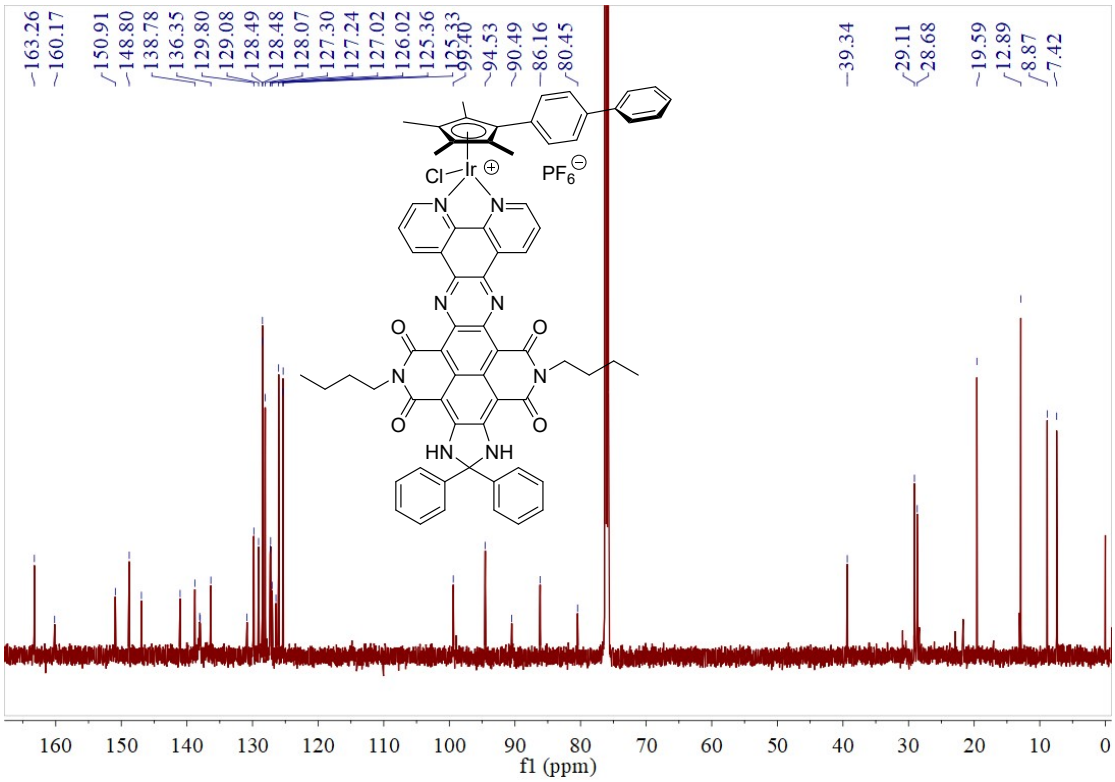

Fig. S6 ^{13}C NMR spectrum of **Ir-NDI** in $CDCl_3$.

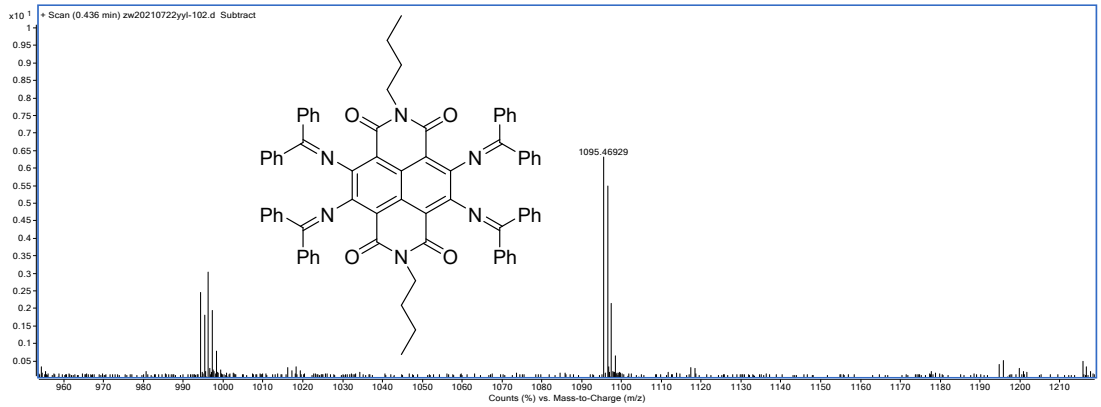

Fig. S7 HR-MS diagram of **4NNDI**.

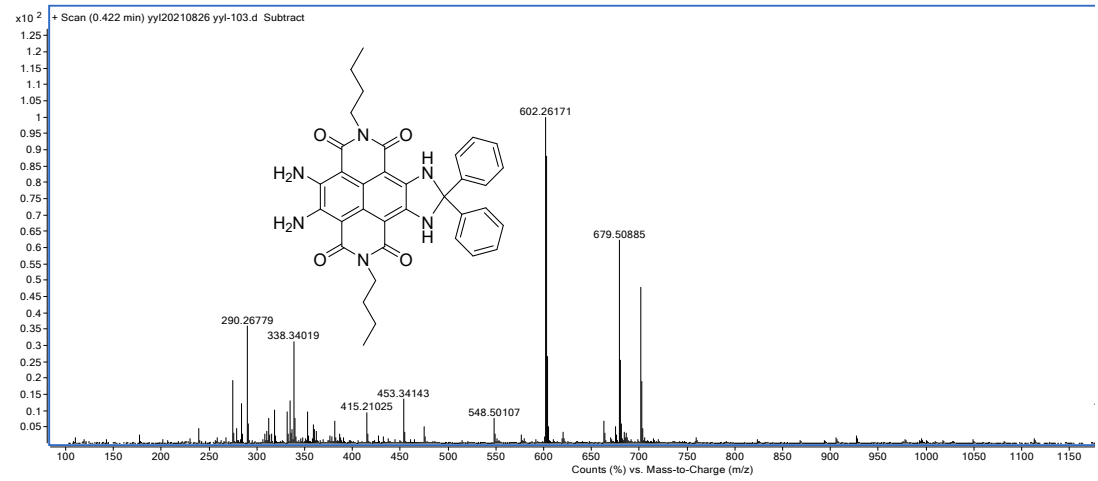

Fig. S8 HR-MS diagram of **2NH$_2$-NDI**.

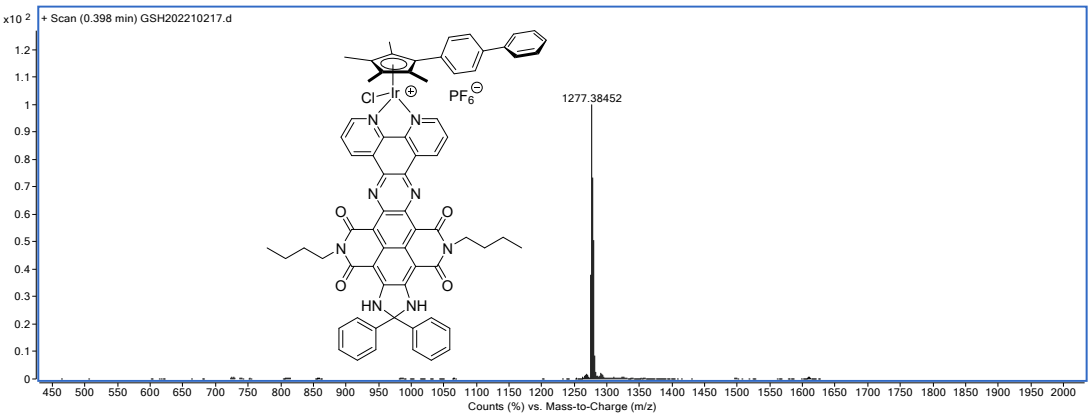

Fig. S9 HR-MS diagram of **Ir-NDI**.

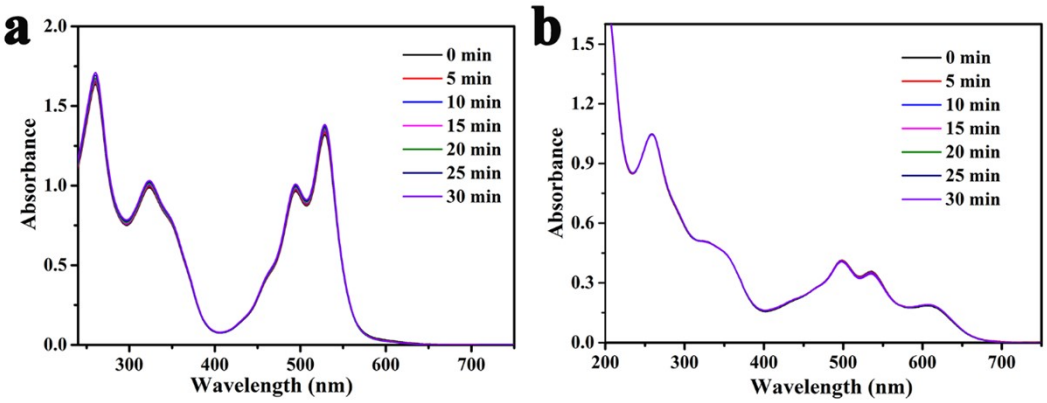

Fig. S10 Photostability study. The absorption spectra of **Ir-NDI** in (a) methanol solution or (b) aqueous solution (with 10% volume of MeOH) after subjecting to 635 nm laser irradiation for different time (145 mW cm^{-2}).

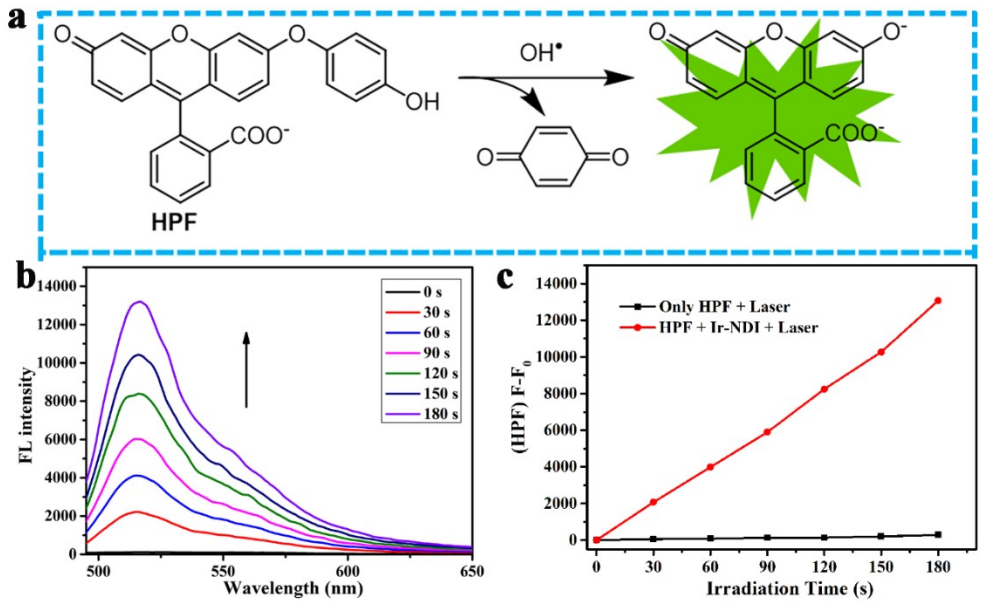

Fig. S11 (a) Schematic illustrations of the detection of •OH using HPF as a probe. (b) The emission spectra of HPF (50 μM, λ_{ex} = 480 nm, λ_{em} = 495-700 nm) in water solution (with 5 vol % MeOH) after irradiation (635 nm, 145 mW cm^{-2}) for different time in the presence of **Ir-NDI** (20 μM). (c) Plots of ΔFl.($F-F_0$) of HPF at 518 nm upon light irradiation for different time intervals in the presence of **Ir-NDI**.

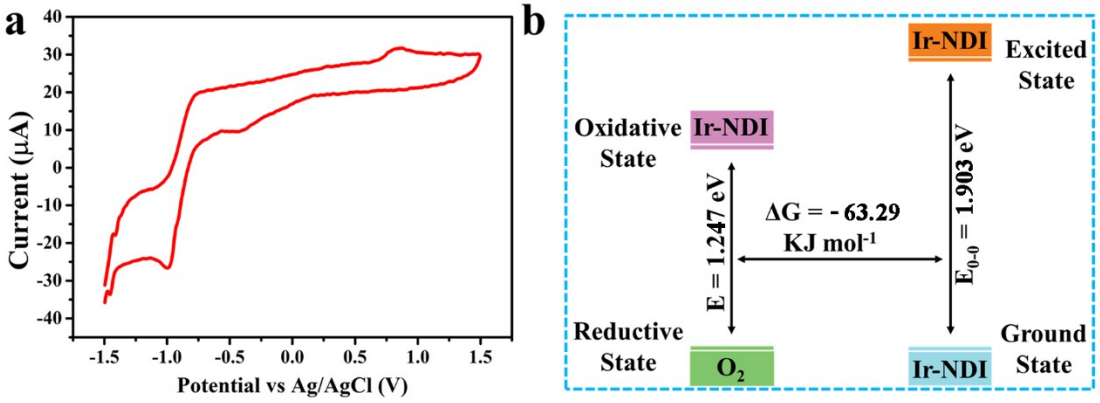

Fig. S12 (a) Cyclic voltammetry data of **Ir-NDI**. (b) Gibbs free energy changes of **Ir-NDI**.

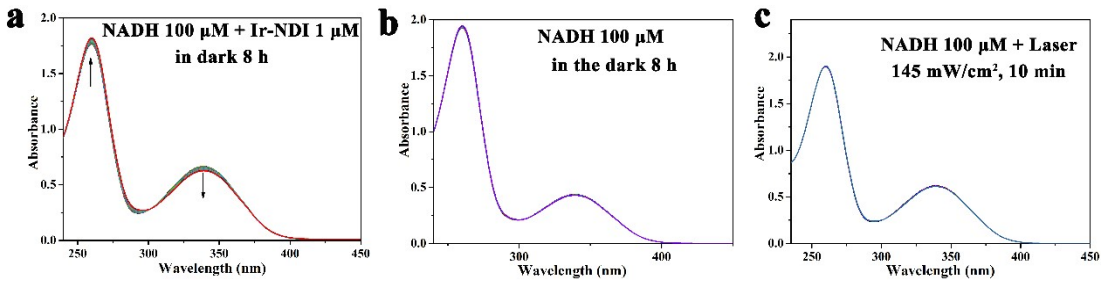

Fig. S13 UV/vis spectra of the reaction of **Ir-NDI** with NADH in 5% MeOH/95% H_2O (v/v) at 298 K. (a) **Ir-NDI** (1 μM) + NADH (100 μM) in the dark for 8 h. (b) NADH (100 μM) in the dark for 8 h; (c) NADH (100 μM) illuminated by 635 nm laser (145 mW cm^{-2}) for 10 min.

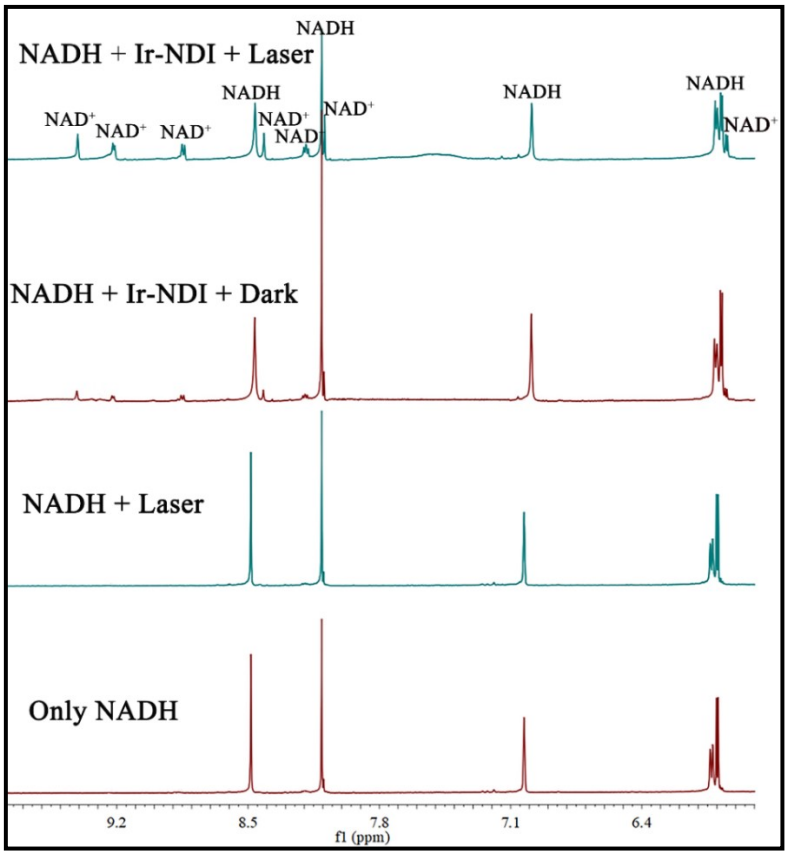

Fig. S14 ^{1}H NMR spectra of the photocatalytic oxidation of NADH (3.5 mM) by **Ir-NDI** (5 μM) in CD_3OD/D_2O (4: 1, v/v) after 10 min light irradiation (365 nm, 145 mW cm^{-2}) or leave it in the dark for 1 h.

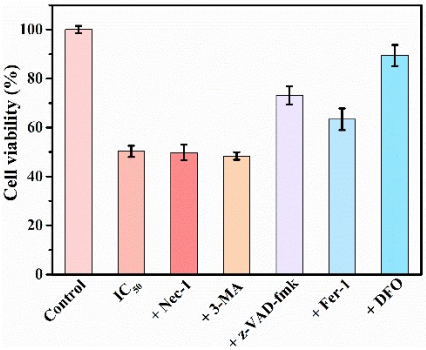

Fig. S15 Cell viability of 4T1 cells pre-incubated with various cell death mechanism inhibitors (z-VAD-FMK: 20 μM, Nec-1: 60 μM, Fer-1: 10 μM, DFO 10 μM, 3-MA 100 μM) and then incubated with **Ir-NDI** and exposed to irradiation (635 nm, 145 mW cm^{-2}, 10 min). Mean ± s.d. (*n* = 3).

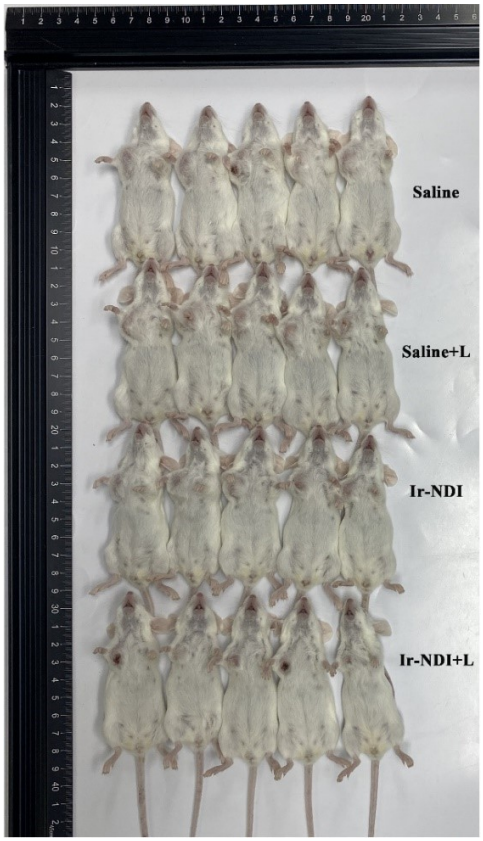

Fig. S16 Images of the mice after various treatments for 21 days.

Table S1 E^{ox}, E^{ox} *vs* NHE and $E_{0\text{-}0}$ for **Ir-NDI**.

Compound	E^{ox} [eV]	E^{ox} *vs* NHE [eV][a]	$E_{0\text{-}0}$[b]
Ir-NDI	0.869	1.047	1.903

[a]E^{ox} *vs* NHE = E^{ox} – $E_{1/2}(F_C^+/F_C)$ + 0.64 eV, $E_{1/2}(F_C^+/F_C)$ was 0.462 eV vs Ag/AgCl; [b]$E_{0\text{-}0}$ is the energy of the lowest excited states calculated by time-dependent density functional theory (TD-DFT) calculations.

References

1. K. K. Wen, H. Tan, Q. Peng, H. Chen, H. Ma, L. Wang, A. D. Peng, Q. Q. Shi, X. D. Cai and H. Huang, Achieving efficient NIR-II Type-I photosensitizers for photodynamic/photothermal therapy upon regulating chalcogen elements, *Adv. Mater.*, 2022, **34**, 2108146.